Mineralogical Magazine, February 2006, Vol. 70(1), pp. 115–121

Crystal structure of a synthetic aluminoan tantalian titanite: a reconnaissance study

R. P. LIFEROVICH† AND R. H. MITCHELL*

Department of Geology, Lakehead University, 955 Oliver Road, Thunder Bay, Ontario, Canada P7B 5E1

ABSTRACT

A synthetic analogue, $Ca(Ti_{0.6}Al_{0.2}Ta_{0.16}Nb_{0.04})OSiO_4$, of an aluminoan tantalian titanite previously described from Craveggia pegmatite (Piemonte, Italy) has been prepared by a ceramic synthesis technique and its crystal structure determined by Rietveld analysis of the powder X-ray diffraction pattern. The synthetic Al-Ta-Nb-rich titanite adopts space group *A*2/*a* implying that substitutions at the single octahedral site destroy the coherence of the off-centering of octahedral chains in the titanite structure resulting in a $P2_1/a \rightarrow A2/a$ phase transition. Unit-cell dimensions obtained for the Al-Ta-Nb-rich titanite are: a = 7.0649(1) Å; b = 8.7187(1) Å; c = 6.5701(1) Å; ß = 113.755(1)º, V = 370.41(1) Å^3. The extensive replacement of Ti by Al, Ta and Nb results in a considerable decrease in the distortion of all coordination polyhedra in the structure of this titanite. These structural data suggest that a solid solution $CaTi_{1-x}(Al_{x/2}[Ta,Nb]_{x/2})OSiO_4$ ($0 \leqslant x \leqslant 0.4$) adopting the titanite structure might exist.

KEYWORDS: titanite, Rietveld analysis, crystal structure, distortion, tantalum, niobium, aluminium.

Introduction

TANTALUM and niobium are less common minor constituents of natural titanite, $^{VII}X^{VI}YOSiO_4$, where X = Ca, Na, *REE*, Y, Sr, Mn, and Y = Ti, Sn, Sb, Al, Fe, Zr, Ta, Nb (Sahama, 1946; Černý and Riva di Sanseverino, 1972; Clark, 1974; Černý *et al*., 1981; Sawka *et al*., 1984; Woolley *et al*., 1992; Della Ventura *et al*., 1999; Tiepolo *et al*., 2002; Chakhmouradian and Zaitsev, 2002; Chakhmouradian *et al*., 2003; Chakhmouradian, 2004). Tantalian and niobian varieties of titanite occur in siliceous pegmatites and in highly-evolved silica-undersaturated rocks, respectively (Černý *et al*., 1981; Chakhmouradian *et al*., 2003; Chakhmouradian, 2004). Entry of $(Ta,Nb)^{5+}$ to the titanite structure at the ^{VI}Y site is commonly balanced by $(Al,Fe)^{3+}$ or by the replacement of Ca^{2+} by Na^+ at the ^{VII}X site. One of the most tantalian titanites known to date contains 16.0 wt.% Ta_2O_5 and 2.9 wt.% Nb_2O_5 and has the empirical formula $(Ca_{0.99}Na_{0.02})_{\Sigma=1.01}(Ti_{0.60}Al_{0.16}Ta_{0.16}Nb_{0.05}Fe_{0.03})_{\Sigma=1}O(Si_{0.97}Al_{0.4})_{\Sigma=1.01}O_4$ (Clark, 1974). This titanite was described as inclusions in holotype strüverite from the pegmatite occurring at Craveggia, Piemonte, Italy [#BM. 1906, 123 as in Clark (1974)]. The highest (Ta,Nb) content ever encountered in titanite was reported by Černý *et al*. (1995) in samples from Maršíkov II pegmatite in northern Moravia, Czech Republic, where up to 21.5 wt.% Ta_2O_5 combines with Al, and also Na, Sn, Fe and F.

The study of the crystal structure of natural Nb-Ta-rich titanites, is typically hindered by their compositional inhomogeneity; thus, their crystal chemistry remains speculative. This contribution provides experimental data regarding the synthesis and stability at ambient conditions of Al-Ta-Nb-rich titanite, and describes the response of the titanite structure to the occupancy of two fifths of the octahedral positions at the *Y*-site by Ta, Nb and Al, as described by Clark (1974).

* E-mail: rmitchell@lakeheadu.ca
DOI: 10.1180/0026461067010317
† Permanent address: Geological Institute KSC RAS, 14 Fersmana St., Apatity, 184200 Russia

The structure of titanite

The structure of titanite consists of kinked chains of corner-linked YO_4O_2 octahedra sharing O(1) atoms (Fig. 1). The SiO_4 tetrahedra cross-link the octahedral chains. Irregular XO_7 polyhedra form interlacing chains sharing edges *via* couples of oxygen atoms and extend down [101]. The YO_6 and XO_7 chains are interconnected by shared edges. The titanite structure may be considered as a $[YOSiO_4]^{2-}$ framework with large cavities enclosing *X* atoms (essentially Ca with minor Na, lanthanides, Sr, U and/or vacancies) in irregular seven-fold cages (Speer and Gibbs, 1976; Taylor and Brown, 1976).

At ambient conditions, in $CaTiOSiO_4$, all ^{VI}Ti atoms occur in off-centre positions which are displaced in the same direction within an individual TiO_6 chain, but in opposite directions between neighbouring chains (Fig. 1), resulting in $P2_1/a$ symmetry. According to Kunz and Brown (1995), this displacement of ^{VI}Ti atoms "out of their otherwise regular octahedron coordination" was interpreted on the basis of complex cation-cation repulsions and second-order Jahn-Teller theorem explaining electronic effects occurring around the octahedrally-coordinated cations of this d^0 transition metal. Kek *et al.* (1997) considered ordering of Ca in the ^{VII}X site as another trigger of the antiferroelectric displacement of ^{VI}Ti in the low-temperature $CaTiOSiO_4$.

The phase transition, known for titanite, can be induced by either an increase in pressure and/or temperature (Kunz *et al.*, 1996; Kek *et al.*, 1997; Angel *et al.*, 1999; Kunz *et al.*, 2000), or occurs as a structural response to elemental substitutions involving single YO_6 site, or complex substitutions in the YO_6 + O(1) or XO_7 + YO_6 sites (Higgins and Ribbe, 1976; Speer and Gibbs, 1976; Troitzsch and Ellis, 2002).

The phase transition is known to be stepwise for the $CaTiOSiO_4$ end member. The complete transformation results in centering of the octahedrally-coordinated atoms in the YO_6 polyhedra due to equalization of the *Y*–O(1) and *Y*–O(1)' distances at P = 3.5 GPa or T > 825 K (Kunz *et al.*, 2000; Malcherek, 2001), and in oscillations of the ^{VII}X atom between two positions (Kek *et al.*, 1997). An intermediate non-quenchable transition between 496 K and 825 K (Ghose *et al.*, 1991; Van Heurk *et al.*, 1991; Salje *et al.*, 1993, etc.) results from loss of long-range order and creation of anti-phase boundaries between O(1)–*Y*–O(1)′ dipoles, leaving domains of $P2_1/a$ symmetry on the unit-cell scale, but an overall, pseudo-centred $A2/a$ symmetry on a long-range scale (Taylor and

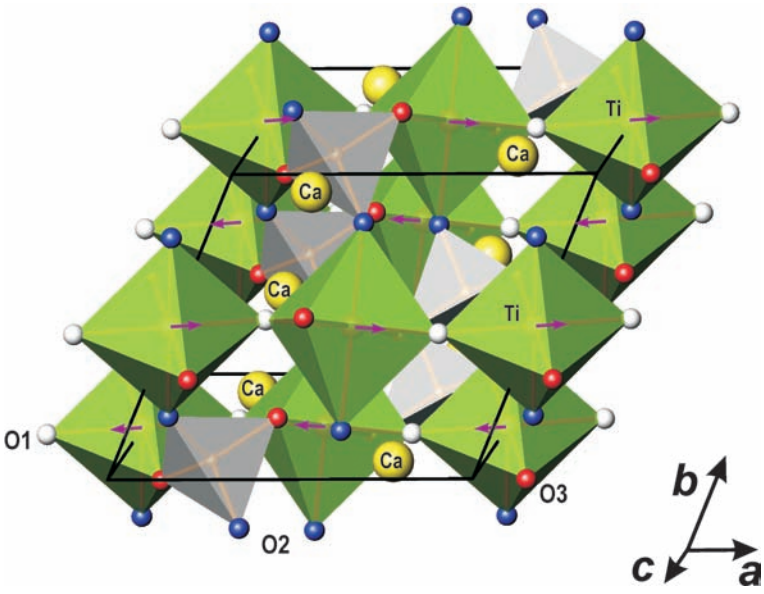

FIG. 1. Crystal structure of aluminoan-tantalian titanite. The lines represent the unit-cell boundaries. Dipoles within TiO_6 octahedra represent off-centre displacement of six-coordinated atoms from the ideal position observed in the $CaTiOSiO_4$ and disappearing in the $CaTi_{0.6}Ta_{0.16}Nb_{0.04}Al_{0.2}OSiO_4$ synthetic titanite.

Brown, 1976; Higgins and Ribbe, 1976; Speer and Gibbs, 1976; Kunz *et al*., 1996; Hughes *et al*., 1997; Troitzsch *et al*., 1999). The ^{VII}X atom is on split position in this intermediate phase (Kek *et al*., 1997). Troitzsch and Ellis (2002) termed the low-temperature phase with space group $P2_1/a$ as "α"-, the intermediate $A2/a$ phase as "β"-, and the high-PT phase with "true $A2/a$ symmetry" as "γ"-titanite. A further temperature-driven phase transition is possible above 1150 K (Chrosch *et al*., 1997). Conventionally, the "$\alpha \rightarrow \beta$" modification is termed "the $P2_1/a$ to $A2/a$ phase transition", bearing in mind that it probably does not strictly represent the entire $P2_1/a \rightarrow A2/a$ transformation (Troitzsch and Ellis, 2002).

In pure $CaTiOSiO_4$, different types of polyhedra have different responses to high pressure and temperature. The SiO_4 tetrahedra show a strong angular distortion with only minor change in bond lengths, whereas the polymerized CaO_7 polyhedra are significantly distorted and TiO_6 octahedra rotate rigidly (Kunz *et al*., 2000).

Compositionally-driven phase transitions of titanite are similar to those driven by high pressure and/or temperature (Troitzsch and Ellis, 2002, and references therein). Doping of the YO_6 site with smaller Al^{3+} ions, balanced by $(F,OH)^-$ in the O(1) site, results in "$\alpha \rightarrow \beta$" transition at low Al+(F,OH) contents and further "$\beta \rightarrow \gamma$"-like modification of more Al-rich titanite (Troitzsch and Ellis, 2002).

Stabilization of the "α"-titanite is possible at ambient conditions by means of entry of as little as 5 mol.% $^{VI}Al^{3+}$ coupled with 5 mol.% charge-balancing $^{VII}Dy^{3+}$ (Hughes *et al*., 1997), whereas in the case of octahedral substitutions balanced by equal amount of F^- at the O(1) site, the "β" dimorph becomes stable for $\geqslant$9 mol.% of the Al^{3+} (Troitzsch *et al*., 1999).

Experimental and analytical technique

Al-Ta-Nb-doped titanite (henceforth 'TIT-Clark') was synthesized by melting a mixture of stoichiometric amounts of oven-dried $CaSiO_3$, TiO_2, Al_2O_3, Ta_2O_5 and Nb_2O_5 at 1475ºC, cooling the melt slowly to 1175ºC and quenching. A pure titanite ($CaTiOSiO_4$) was prepared by solid-state ceramic techniques as a reference material. The synthetic compounds were investigated by Energy-Dispersive X-ray Spectrometry (EDXA) using a JEOL JSM-5900 scanning electron microscope equipped with a Link ISIS 300 analytical system. Raw EDS spectra were acquired for 130 s (live time) with an accelerating voltage of 20 kV, and beam current of 0.475 nA. The spectra were processed with the LINK ISIS-SEMQUANT quantitative software package, with full ZAF corrections applied. The following well-characterized mineral and synthetic compounds were used as analytical standards: corundum (Al), ilmenite (Fe, Ti), wollastonite (Ca), pyroxene glass DJ35 (Si), natural lueshite (Nb), and metallic Ta (Ta).

Powder X-ray diffraction (XRD) patterns were obtained at room temperature using a Philips 3710 diffractometer (T = 20ºC; Cu-$K\alpha$ radiation; 2θ range 9–145º, Δ2θ step 0.02º per 4 s). The patterns were analysed by the Rietveld method using the Bruker AXS software TOPAS 2.1 (Kern and Coelho, 1998). In addition, high-resolution XRD patterns were obtained in the 2θ range 31.7–33.4º (Δ2θ step 0.005º; counting time per step – 30 s). The occupancies of Ca(1) and Si(1) sites were set to 1, and that of the octahedral site set in accord with the composition as determined by EDXA. Refinement of occupancies of the Ca(1), Y(1) and Si(1) sites converges to values approaching $1.0Ca^{2+}$, $[0.6Ti^{4+} + 0.16Ta^{5+} + 0.04Nb^{5+} + 0.20Al^{3+}]$ and $1.0Si^{4+}$, within accuracy of the Rietveld refinement method.

The ATOMS-5.0 software (Dowty, 1999) was used to determine interaxial angles. The IVTON program (Balić-Žunić and Vicković, 1996) was employed to obtain selected bond lengths and characterize the coordination spheres of the cations.

Results and discussion

No significant compositional heterogeneity was observed in the synthesized titanites and within analytical error these are considered to be $CaTiOSiO_4$ and $CaTi_{0.6}Al_{0.2}Ta_{0.16}Nb_{0.04}OSiO_4$ ('TIT-Clark'). The latter consists of [wt.%]: 28.2(6) SiO_2, 25.8(3) CaO, 22.2(3) TiO_2, 16.6(7) Ta_2O_5, 4.6(2) Al_2O_3, and 2.4(3) Nb_2O_5.

Rietveld refinement

For the Al-Ta-Nb-doped variety of synthetic titanite ('TIT-Clark'), high-resolution laboratory powder XRD does not indicate the presence of $2\bar{2}\bar{1}$ and $2\bar{1}\bar{2}$ reflections, which occur clearly in the high-resolution XRD pattern of the pure $CaTiOSiO_4$ end-member (cf. Fig. 2). Given that extinction rules do not allow these $k + l$ = odd reflections in the space group $A2/a$, we conclude that doping of the octahedral site of the titanite

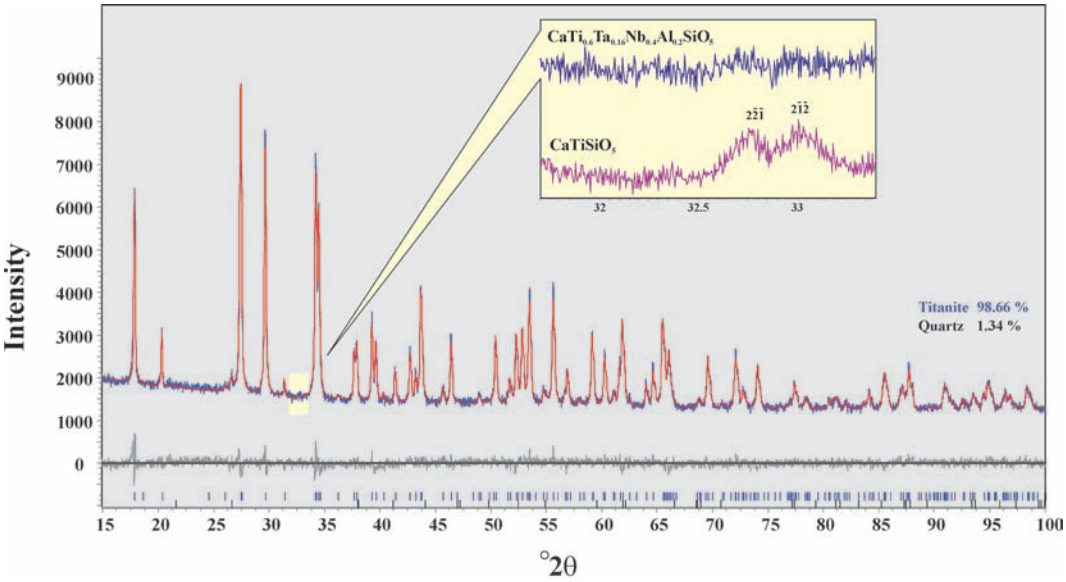

FIG. 2. A portion of the Rietveld refinement plot of the X-ray powder diffraction data for $CaTi_{0.6}Ta_{0.16}Nb_{0.04}Al_{0.2}OSiO_4$ synthetic titanite at room temperature. The bars indicate the allowed Bragg reflections for primitive titanite structure. For details of the refinement, see the text and Table 2. High-resolution details are provided to demonstrate the absence of the $2\bar{2}\bar{1}$ and $2\bar{1}\bar{2}$ reflections on the powder XRD pattern of the $CaTi_{0.6}Ta_{0.16}Nb_{0.04}Al_{0.2}OSiO_4$ titanite and their presence on that of the $CaTiOSiO_4$ titanite.

structure with Al-Ta-Nb at ambient pressure results in the stabilization of an *A*2/*a* dimorph. We did not observe any superlattice reflections which might imply ordering of Ti^{4+}, Ta^{5+}, Nb^{5+} and Al^{3+} cations at the octahedral site. Figure 2 is a Rietveld refinement plot for the Al-Ta-Nb-rich titanite, which is found to contain minor ($\approx$1.3 wt.%) SiO_2 as an impurity phase (not recognized by SEM technique); this impurity is considered to have been introduced by use of an agate mortar during sample preparation. Atom positions and isotropic thermal parameters obtained for this sample are listed in Table 1; refinement parameters, unit-cell parameters, and coordination polyhedra distortion parameters are given in Table 2; and bond lengths and selected framework bond angles within the coordination polyhedra are listed in Table 3.

TABLE 1. Positional and thermal parameters of synthetic Al-Ta-Nb-rich titanite at ambient conditions.

			TIT-Clark		
	x	*y*	*z*	SoF	B_{iso} (Å^2)
^{VII}Ca	¼	0.1695(3)	0	1	2.11(1)
^{VI}*Y*	½	0	½	0.60 Ti 0.16 Ta 0.04 Nb 0.20 Al	0.61(4)
^{IV}Si	¾	0.1808(5)	0	1	0.93(11)
O1	¾	0.0667(7)	½	1	1.22(8)
O2	0.9118(7)	0.0659(5)	0.1822(6)	1	1.22(8)
O3	0.3854(6)	0.2104(5)	0.4034(8)	1	1.22(8)

TIT-Clark $CaTi_{0.60}Ta_{0.16}Nb_{0.04}Al_{0.20}OSiO_4$

TABLE 2. Rietveld refinement results and crystal structure parameters of synthetic titanite.

	$CaSiOTiO_4$	TIT-Clark		$CaSiOTiO_4$	TIT-Clark
a (Å)	*7.0599(1)*	7.0649(1)	<X–O> (Å)	*2.463(12)*	2.467(5)
b (Å)	*8.7156(1)*	8.7187(1)	V_{XO7} (Å^3)	*19.887 (20)*	20.087(9)
c (Å)	*6.5597(1)*	6.5701(1)	Δ_7	*2.90*	1.76
ß (º)	*113.797(1)*	113.755(1)	υ_7	*0.157*	0.155
V (Å^3)	*369.30(1)*	370.41(1)	<Y–O> (Å)	*1.966(14)*	1.956(4)
			V_{YO6} (Å^3)	*10.095(15)*	9.960(4)
R_{wp} (%)	*11.50*	7.65	d_Y	*0.060*	0.0
R_{Bragg} (%)	*3.01*	2.67	∂_{xY}	*0.009*	–
GoF	*1.31*	1.32	∂_{yY}	*0.000*	–
DW	*1.26*	1.25	∂_{zY}	*0.003*	–
			Δ_6	*2.35*	1.21
			υ_6	*0.004*	0.002
Ti–O1–Ti (º)	*143.2*	143.5	<Si–O> (Å)	*1.622(14)*	1.635(5)
Si–O2–Ti (º)	*142.5*	140.7	V_{SiO4} (Å^3)	*2.177(12)*	2.226(4)
Si–O3–Ti (º)	*139.5*	129.0	Δ_4	*0.19*	0.04
Si–O4–Ti (º)	*130.1*		υ_4	*0.007*	0.008
Si–O5–Ti (º)	*128.1*		δ_6	*2.56*	1.19
			δ_4	*17.24*	19.31

$CaTiOSiO_4$ titanite end-member (this study); TIT-Clark $CaTi_{0.60}Ta_{0.16}Nb_{0.04}Al_{0.20}OSiO_4$.
d_Y: The displacement of the central atom; ∂_{xY}, ∂_{yY} and ∂_{zY} components of the vector of ^{VI}Y atom displacement;
Δ_n: Polyhedron bond length distortion, $\Delta_n = \frac{1}{n}\cdot\Sigma\{(r_i - \bar{r})/\bar{r}\}^2\cdot 10^3$, where r_i and $\bar{r}$ are individual and average bond lengths, respectively (Shannon, 1976);
υ_n: Polyhedron volume distortion calculated relative to an ideal polyhedron with the same coordination number and inscribed in the sphere with the radius r_s (average distance from centroid to ligands [Makovicky and Balić-Žunić, 1998; Balić-Žunić and Vicković, 1996]).
δ_n: Bond angle variance in for the regular polyhedra, $\delta_n = \Sigma[(\theta_i - \varphi_j)^2/(n-1)]$ where θ_i are bond angles and φ_j is an ideal bond angle (Robinson *et al*., 1971).
Parameters for $P2_1/a$-structured compound are given in italics

TABLE 3. Selected refined bond-lengths of synthetic titanite varieties.

	$CaSiOTiO_4$		TIT-Clark		$CaSiOTiO_4$		TIT-Clark
Ca–O1	*2.293(5)*	X–O1	2.300(6)	Ti–O1	*1.755(14)*	2 × Y–O1	1.860(2)
Ca–O2	*2.430(12)*	2 × X–O2	2.418(5)	Ti–O1′	*1.978(14)*	2 × Y–O2	2.002(4)
Ca–O3	*2.402(12)*	2 × X–O3	2.455(5)	Ti–O2	*2.011(15)*	2 × Y–O3	2.007(4)
Ca–O4	*2.394(14)*	2 × X–O3′	2.612(6)	Ti–O3	*2.007(15)*		
Ca–O4’	*2.752(12)*			Ti–O4	*2.024(13)*		
Ca–O5	*2.471(15)*			Ti–O5	*2.018(13)*		
Ca–O5’	*2.499(12)*						
				Si–O2	*1.619(12)*	2 × Si–O2	1.625(5)
				Si–O3	*1.602(12)*	2 × Si–O3	1.646(6)
				Si–O4	*1.608(16)*		
				Si–O5	*1.659(16)*		

$CaTiOSiO_4$ titanite end-member (this study); TIT-Clark $CaTi_{0.60}Ta_{0.16}Nb_{0.04}Al_{0.20}OSiO_4$.
Parameters for $P2_1/a$-structured compounds are given in italics.

Crystal structure of Nb-Ta-Al-rich titanite

Unit-cell parameters obtained for synthetic pure titanite (Table 2) are close to those given by Kek *et al*. (1997). The average atomic radius of $^{VI}R_{(0.60Ti+0.20Al+0.16Ta+0.04Nb)}$ = 0.6 Å in the 'TIT-Clark' titanite, is slightly smaller than $^{VI}R_{Ti^{4+}}$ = 0.605 Å (Shannon, 1976), nevertheless, this compound has slightly larger unit-cell dimensions compared to $CaTiOSiO_4$ titanite (Table 2). The mean distances within the coordination polyhedra are similar in both compounds. Bond-length distortion parameters (Table 2) show that entry of Al, Ta and Nb to the octahedral site mitigates distortion of the seven-fold CaO_7, octahedral YO_6, and tetrahedral SiO_4 sites. Bond-angle variance parameters are less for both tetrahedra and octahedra in the TIT-Clark titanite (Table 2). The kinking of the chains of octahedra, as shown by the pivoting Ti–O(1)–Ti angle (Table 2), is essentially unaffected by substitution of two fifths of Ti by Al+Ta+Nb.

Conclusion

This work demonstrates that titanite with substitution of 40% $^{VI}Ti^{4+}$ by ^{VI}(Al+Ta+Nb) is stable at ambient pressure and adopts the space group *A*2/*a*. In contrast to the pure titanite end-member, ^{VI}Y atoms in the crystal structure of the Al-Ta-Nb-rich titanite are not displaced from the centres of octahedra and/or do not retain long-distance coherency in their displacement within the chains of the YO_6 octahedra (Fig. 1). Nevertheless, any conclusions regarding the nature of centering of the ^{VI}Y atom and thus discrimination between the *A*2/*a*-structured "β" and "γ" phases introduced by Troitzsch and Ellis (2002), are not possible on the basis of routine powder XRD techniques. The similarity of the average ionic radius of the ^{VI}[Al+Ta+Nb] to that of $^{VI}Ti^{4+}$ results in a $CaTi_{1-x}(Al_{x/2}[Ta,Nb]_{x/2})OSiO_4$ solid solution extending to at least x = 0.4, and consisting of less-distorted coordination polyhedra as compared with the $CaTiOSiO_4$ end-member. The synthesis and stability of the (OH,F)-free Nb-Ta-Al-rich titanite at ambient pressure implies that the Ta-rich titanite described by Clark (1974) and coeval strüverite from the Craveggia pegmatite (Piemont, Italy) might be of low-pressure origin and could form under low fugacities of volatile components.

The Ti^{4+}, $(Ta,Nb)^{5+}$ and Al^{3+} cations, which are of different size (Shannon, 1976), are randomly distributed at the available octahedral site. Thus, the $2\,^{VI}Ti^{4+} \rightarrow {}^{VI}(Ta,Nb) + {}^{VI}Al^{3+}$ substitutional scheme does not induce long-range ordering, at least at a level recognizable by routine powder XRD. Our study provides experimental confirmation that the structure of titanite is capable of hosting significant amounts of high-field strength elements (HFSE) and substitutions of up to 40% at the octahedral site. These substitutions reduce the distortion of the coordination polyhedra in the structure thus suggesting that titanite might host significantly larger amounts of Ta and Nb. This observation also implies that OH-F-free titanite-structured solids might possibly be employed for long-term safe disposal of HFSE, including radionucleids.

Acknowledgements

This work is supported by the Natural Sciences and Engineering Research Council of Canada and Lakehead University (Canada). We are grateful to Allan MacKenzie for assistance with the analytical work, and Anne Hammond for sample preparation. Constructive criticism by anonymous reviewers resulted in improvements to the initial version of this work. The authors also thank Dr Mark Welch for editorial care in handling of this contribution.

References

Angel, R.J., Kunz, M., Miletich, R., Woodland, A.B., Koch, M. and Xirochakis, D. (1999) High-pressure phase transitions in $CaTiOSiO_4$ titanite. *Phase Transitions*, **68**, 533–543.

Balić-Žunić, T. and Vicković, I. (1996) IVTON – a program for the calculation of geometrical aspects of crystal structures and some crystal chemical applications. *Journal of Applied Crystallography*, **29**, 305–306.

Černý, P. and Riva di Sanseverino, L. (1972) Comments on crystal chemistry of titanite. *Neues Jahrbuch für Mineralogie Monatshefte*, 97–103.

Černý, B.J., Chapman, R. and Hinthorne, J.R. (1981) Niobian titanite from the Huron claim pegmatite, southeastern Manitoba. *The Canadian Mineralogist*, **19**, 549–552.

Černý, P., Novák, M. and Chapman, R. (1995) The Al(Nb,Ta)Ti_{-2} substitution in titanite: the emergence of a new species? *Mineralogy and Petrology*, **52**, 61–73.

Chakhmouradian, A.R. (2004) Crystal chemistry and paragenesis of compositionally-unique (Al-, Fe-, Nb-, and Zr-rich) titanite from Africanda, Russia. *American Mineralogist*, **89**, 1752–1762.

Chakhmouradian, A.R. and Zaitsev, A.N. (2002) Calcite-amphibole-clinopyroxene rock from Afrikanda Complex, Kola peninsula, Russia: mineralogy and possible link to carbonatites. III. Silicate minerals. *The Canadian Mineralogist*, **40**, 1347–1374.

Chakhmouradian, A.R., Reguir, E.P. and Mitchell, R.H. (2003) Titanite in carbonatitic rocks: Genetic dualism and geochemical significance. *Periodico di Mineralogia*, **72** Eurocarb Special Issue, 107–113.

Chrosch, J., Bismayer, U. and Salje, E.K.H. (1997) Anti-phase boundaries and phase transitions in titanite: An X-ray diffraction study. *American Mineralogist*, **82**, 677–681.

Clark, A.M. (1974) A tantalum-rich variety of sphene. *Mineralogical Magazine*, **39**, 605–607.

Della Ventura, G., Bellatreccia, F. and Williams, C.T. (1999) Zr- and *LREE*-rich titanite from Tre Croci, Vico Volcanic complex (Latinum, Italy). *Mineralogical Magazine*, **63**, 123–130.

Dowty, E. (1999) *Atoms 5.0*. By Shape Software, Kingsport, TN 37663, USA, http://shapesoftware.com/

Ghose, S., Yoshiaki, I. and Hatch, D.M. (1991) Paraelectric-antiferroelectric phase transition in titanite, $CaTiSiO_5$. I. A high-temperature X-ray diffraction study of the order parameter and transition mechanism. *Physics and Chemistry of Minerals*, **17**, 591–603.

Higgins, J.B. and Ribbe, P.H. (1976) The crystal chemistry and space groups of natural and synthetic titanites. *American Mineralogist*, **61**, 878–888.

Hughes, J.M., Bloodaxe, E.S., Hanchar, J.M. and Foord, E.E. (1997) Incorporation of rare earth elements in titanite: Stabilization of the *A2/a* dimorph by creation of antiphase boundaries. *American Mineralogist*, **82**, 512–516.

Kek, S., Aroyo, M., Bismayer, U., Schmidt, C., Eichhorn, K. and Krane, H.G. (1997) The two-step phase transition of titanite, $CaTiSiO_5$: a synchrotron radiation study. *Zeitschrift für Kristallographie*, **212**, 9–19.

Kern, A.A. and Coelho, A.A. (1998) *TOPAS*. Allied Publishers Ltd. http://www.bruker-axs.com.

Kunz, M. and Brown, I.D. (1995) Out-of-center distortions around octahedrally coordinated d^0-transition metals. *Journal of Solid State Chemistry*, **115**, 395–406.

Kunz, M., Xirouchakis, D., Lindsley, D.H. and Häusermann, D. (1996) High-pressure phase transition in titanite ($CaTiOSiO_4$). *American Mineralogist*, **81**, 1527–1530.

Kunz, M., Arlt, T. and Stolz, J. (2000) In situ powder diffraction study of titanite ($CaTiOSiO_4$) at high pressure and high temperature. *American Mineralogist*, **85**, 1465–1473.

Makovicky, E. and Balić-Zunić, T. (1998) New measure of distortion for coordination polyhedra. *Acta Crystallographica*, **B54**, 766–773.

Malcherek, T. (2001) Spontaneous strain in synthetic titanite, $CaTiOSiO_4$. *Mineralogical Magazine*, **65**, 709–715.

Robinson, K., Gibbs, G.V. and Ribbe, P.H. (1971) Quadratic elongation: a quantitative measure of distortion in coordination polyhedra. *Science*, **172**, 567–570.

Sahama, Th.G. (1946) On the chemistry of mineral titanite. *Bulletin Committee Géologia Finlandie*, **24**, **138**, 88–120.

Salje, E., Schmidt, C. and Bismayer, U. (1993) Structural phase transitions in titanite, $CaTiSiO_5$: a Raman spectroscopic study. *Physics and Chemistry of Minerals*, **19**, 502–506.

Sawka, W.N., Campbell, R.B. and Norrish, K. (1984) Light-rare-earth-element zoning in sphene and allanite during granitoid fractionation. *Geology*, **12**, 131–134.

Shannon, R.D. (1976) Revised effective ionic radii and systematic studies of interatomic distances in halides and chalcogenides. *Acta Crystallographica*, **A32**, 751–767.

Speer, J.A. and Gibbs, G.V. (1976) The crystal structure of synthetic titanite, $CaTiOSiO_4$, and the domain textures of natural titanites. *American Mineralogist*, **61**, 238–247.

Taylor, M. and Brown, G.E. (1976) High-temperature structural study of the $P2_1/a \rightarrow A2/a$ phase transition in synthetic titanite, $CaTiSiO_5$. *American Mineralogist*, **61**, 435–437.

Tiepolo, M., Oberti, R. and Vanucci, R. (2002) Trace-element incorporation in titanite: constraints from experimentally determined solid/liquid partition coefficients. *Chemical Geology*, **191**, 105–119.

Troitzsch, U. and Ellis, D.J. (2002) Thermodynamic properties and stability of AlF-bearing titanite $CaTiOSiO_4$-$CaAlFSiO_4$. *Contributions to Mineralogy and Petrology*, **142**, 543–563.

Troitzsch, U., Ellis, D.J., Thompson, J. and FitzGerald, J.D. (1999) Crystal structural changes in titanite along the join TiO-AlF. *European Journal of Mineralogy*, **6**, 955–965.

Van Heurk, C., van Tendeloo, G., Ghose, S. and Amelinckx, S. (1991) Paraelectric-antiferroelectric phase transition in titanite, $CaTiSiO_5$. II. Electron diffraction and electron microscopic studies of the transition dynamics. *Physics and Chemistry of Minerals*, **17**, 604–610.

Woolley, A.R., Platt, R.G. and Eby, N. (1992) Niobian titanite from the Ilomba nepheline syenite complex, north Malawi. *Mineralogical Magazine*, **56**, 428–430.

[*Manuscript received 13 March 2005: revised 4 November 2005*]